Discerning small time-lapse traveltime changes by isolating the seismic response of a reservoir using the Marchenko method

Johno van IJsseldijk and Kees Wapenaar (Delft University of Technology)*

SUMMARY

4D seismic studies aim to observe time-lapse changes in the subsurface between a baseline and a monitor study. These changes are generally small, and the seismic response from a deep reservoir can be concealed by reflections from shallow structures. Here, we introduce a novel way of isolating the reservoir response by means of the Marchenko method. First, this two-step approach removes the overburden interactions, and the second step eliminates the underburden reflections. Finally, the difference in traveltime is found by correlation of the (isolated) responses of the baseline and monitor study. An additional benefit of isolating the reservoir response is that internal multiples are more distinctly observed. These multiples have propagated through the reservoir more than once, therefore, their response experiences a larger traveltime perturbation, and provides further confirmation on the traveltime difference between the 4D studies.

INTRODUCTION

Geophysical time-lapse methods are an essential part in monitoring reservoirs. Applications range from determining pressure and fluid saturation changes (Landrø, 2001) to monitoring CO_2 injection (Roach et al., 2015) to observing compaction in a reservoir (Hatchell and Bourne, 2005). All these methods capitalize on the observed changes between a baseline and monitor study. These changes can either be a difference in amplitude (e.g. Landrø, 2001), a difference in traveltime (e.g. Landrø and Stammeijer, 2004) or a combination of both (e.g. Trani et al., 2011). However, the efficacy of these monitoring method is hindered, in cases where the reservoir is overlain by a highly scattering overburden with a seismic response that masks the response of the reservoir.

Recently, the Marchenko method was introduced as a data-driven method for redatuming the seismic wavefield, which accounts for all orders of multiples (Wapenaar et al., 2014; Slob et al., 2014). Using this novel method, undesirable overburden effects can be removed from the seismic response. Moreover, the method can be applied a second time to also exclude underburden effects, effectively isolating the reservoir response. Using the isolated primary reflection of the reservoir, the difference in traveltime can be more precisely determined.

In addition to a clearer primary response from the reservoir, the method also reveals internal multiples. These multiples have propagated through the reservoir multiple times, hence they experience a larger time-shift compared to the primary reflection. Inspired by the principle of coda-wave interferometry (Snieder et al., 2002), Wapenaar and Van IJsseldijk (2020) show how these multiples can be used to improve the detectability of traveltime changes.

In this work we develop a method to calculate the traveltime difference in the response of a reservoir situated between a highly reflective over- and underburden, using both primary and multiple reflections. First, the theory used to isolate the reflection response is introduced. Next, a numerical model describing both the baseline and monitor study is presented. The reservoir response is then isolated from full reflection responses of both studies. Finally, the traveltime changes of the primary as well as the multiple reflections are calculated.

THEORY

To start we consider a heterogeneous medium that is divided into three parts: overburden "a", target zone "b", in which the reservoir is situated, and underburden "c". The reflection response due to sources at $\mathbf{x}_S$ measured at receiver positions $\mathbf{x}_R$ is denoted by $R^0_{abc}(\mathbf{x}_R, \mathbf{x}_S, t)$. The superscript 0 denotes that the response is measured at the acquisition surface $\mathbb{S}_0$, and the subscript *abc* indicates that it concerns the entire medium. This wavefield can be redatumed to any level in the subsurface using the Marchenko method.

At the core of the Marchenko method are two coupled representations that read (Wapenaar et al., 2014)

$$G^-(\mathbf{x}, \mathbf{x}_R, t) + f_1^-(\mathbf{x}_R, \mathbf{x}, t) = \int_{\mathbb{S}_0} R^0_{abc}(\mathbf{x}_R, \mathbf{x}_S, t) * f_1^+(\mathbf{x}_S, \mathbf{x}, t) d\mathbf{x}_S, \tag{1}$$

$$G^+(\mathbf{x}, \mathbf{x}_R, t) - f_1^+(\mathbf{x}_R, \mathbf{x}, -t) = -\int_{\mathbb{S}_0} R^0_{abc}(\mathbf{x}_R, \mathbf{x}_S, t) * f_1^-(\mathbf{x}_S, \mathbf{x}, -t) d\mathbf{x}_S. \tag{2}$$

Here, $*$ represents temporal convolution. f_1^+ is a focusing function that focuses the wavefield at focal point $\mathbf{x}$, and f_1^- is its response. Both focusing functions are defined in a truncated medium that is identical to the full medium above the focal level, and homogeneous below the focal level. Furthermore, G^- and G^+ are the up- and down-going Green's functions, respectively, which are excited at $\mathbf{x}_R$ and measured at $\mathbf{x}$. A full derivation of the Marchenko method is beyond the scope of this work, an inquisitive reader is referred to Wapenaar et al. (2014) and Slob et al. (2014).

Subsequently, the Green's functions produced by coupled equations 1 and 2 can be used to redatum the wavefield to focal

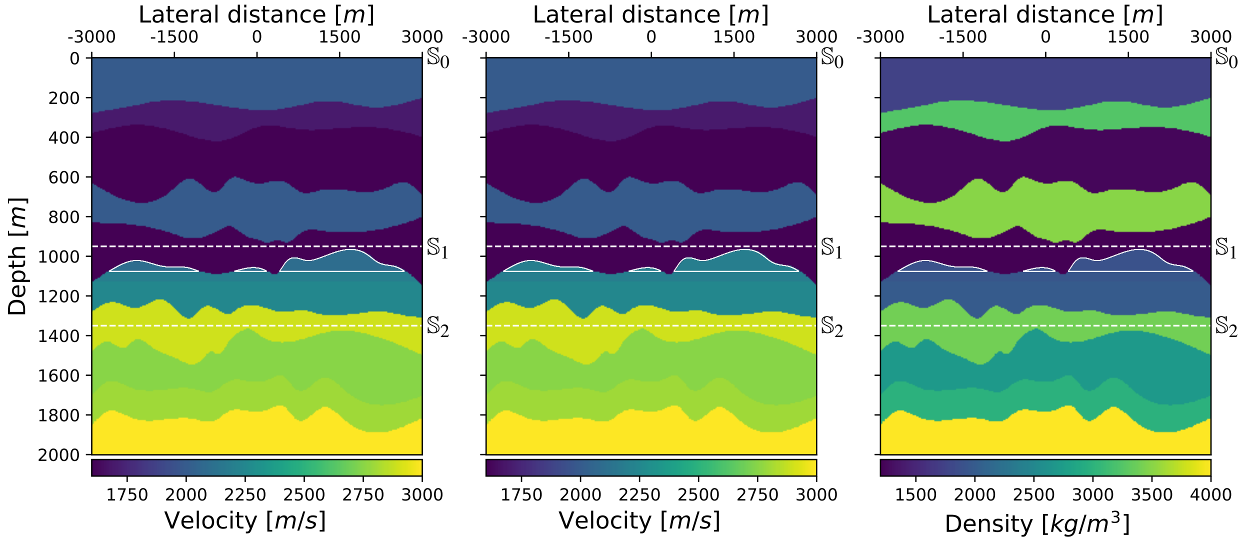

Figure 1: *Velocity model of the baseline (left) and monitor (middle), the density model (right) remains constant over both studies. The white dashed lines represent the two focal depths for the Marchenko method. Lastly, the solid white line highlights the reservoir, where the velocity increases with 100m/s.*

level $\mathbb{S}_1$, which is located at boundary between the overburden "a" and the target zone "b", using:

$$G^-(\mathbf{x},\mathbf{x}_R,t) = \int_{\mathbb{S}_1} R_{bc}(\mathbf{x},\mathbf{x}',t) * G^+(\mathbf{x}',\mathbf{x}_R,t)d\mathbf{x}'. \quad (3)$$

Here, R_{bc} is the reflection response at top of the target zone. Note that this response is measured at focal depth $\mathbb{S}_1$ and not at the acquisition surface. The redatumed response R_{bc} is retrieved from Equation 3 by means of a multi-dimensional deconvolution (MDD, Wapenaar et al., 2011).

The redatumed reflection response is extrapolated upward to the surface by:

$$R^0_{bc}(\mathbf{x}_R,\mathbf{x}_S,t) = \quad (4)$$

$$\int_{\mathbb{S}_1}\int_{\mathbb{S}_1} G_d(\mathbf{x}_R,\mathbf{x},t) * R_{bc}(\mathbf{x},\mathbf{x}',t) * G_d(\mathbf{x}',\mathbf{x}_S,t)d\mathbf{x}d\mathbf{x}'.$$

Here, G_d is the direct arrival of the Green's function between the focal and acquisition surface, which can be modeled in a smooth version of the velocity model. Note that this function is already a prerequisite for the Marchenko scheme, and, therefore, it does not introduce additional constraints to the method. After applying Equation 4, the overburden interactions have effectively been removed from the reflection response, leaving only the responses of the target zone and underburden.

The next step is to remove the underburden, and fully isolate the target zone. In order to achieve this, the Marchenko method is applied for a second time on the newly acquired reflection data (i.e. by replacing R^0_{abc} with R^0_{bc} in equations 1 and 2). A new focal depth $\mathbb{S}_2$ is also defined, located at the interface between target zone "b" and underburden "c". From the resulting focusing functions, a new reflection response can be extracted as follows:

$$f_1^-(\mathbf{x}_R,\mathbf{x},t) = \int_{\mathbb{S}_0} R^0_b(\mathbf{x}_R,\mathbf{x}_S,t) * f_1^+(\mathbf{x}_S,\mathbf{x},t)d\mathbf{x}_S. \quad (5)$$

Similarly to Equation 3, Equation 5 can also be solved using MDD. This time the resulting reflection response is already measured at the acquisition surface $\mathbb{S}_0$ and no further extrapolations are necessary.

Subsequently, the same procedure is applied to the monitor study, thereafter the primary and multiple responses can be identified and separated in order to compute traveltime differences.

MODELING

Now that the theoretical background has been outlined, the methodology will be tested on a numerical example. Figure 1 displays the velocity model of both the baseline and monitor survey. For simplicity the density does not change between the surveys, but this is not a requirement for the method. The solid white line in the figure highlights the position of the reservoir, where the velocity increases with $100m/s$. Moreover, the focal depths are indicated by dashed white lines, $\mathbb{S}_1$ and $\mathbb{S}_2$ mark the interface of target zone "b" with overburden "a" and underburden "c", respectively. One might notice that within the target zone an additional reflector (at $\sim 1250m$) is included, this ensures that the isolated response will contain energy that has propagated through the reservoir at least once.

The initial baseline and monitor responses are modeled using a wavelet with a flat spectrum between 5 and 80 Hz. The wavefield is excited by 601 sources, with a spacing of 10 meters, and recorded by the same number of receivers with a sampling rate of 4*ms*. Furthermore, the direct arrivals of the Green's functions (at depths 950*m* and 1350*m*) used for Equation 4 and the Marchenko method are computed in a smooth version of the baseline velocity and density model.

Using the direct arrivals of the Green's functions and the reflection response of the full medium, 2 additional reflection responses for both the baseline and monitor study are retrieved with the Marchenko method; R^0_{bc} encompassing the medium below $\mathbb{S}_1$, and R^0_b solely containing the target zone response. Finally, the zero-offset trace from each retrieved shot is extracted for the computation of the traveltime differences. Note that by only examining the zero-offset traces, we tacitly assume that we can solve the traveltime difference as a 1D problem below each virtual source-receiver location.

RESULTS

The time-lapse analysis is started by determining the arrival times of the first and second primary in the target zone, this is most easily achieved by examining R^0_b, where both primaries are clearly isolated. Next, the arrival times of the internal multiples can be computed from these primaries. A correlation window is then defined around the desired reflection, as shown in the top row of Figure 2, where the red and blue zones mark the correlation windows around the second primary and first multiple, respectively. The final step is to resolve the traveltime difference in the reservoir, by correlating the baseline and monitor response inside of the window.

Before correlation, interpolation by padding with zeros in the frequency domain is applied to both responses. This allows for increased resolution beyond the sampling rate of 4*ms*. Subsequently, the windowed baseline response is cross-correlated with the same window of the monitor response, and the argument of the maximum of this correlation determines the traveltime difference at each receiver location. Finally, the traveltime differences are smoothed over the whole receiver array by means of a Gaussian filter.

Figures 2D and E show the resulting time differences at each location for the numerical example. First, in Figure 2D the results for the second primary are displayed. The dashed blue, dotted orange and solid green lines represent the correlation results for R^0_{abc}, R^0_{bc} and R^0_b, respectively. Moreover, the light blue background highlights the actual difference in traveltime below each receiver. The correlations of R^0_{bc} and R^0_b clearly capture the actual difference, whereas the the correlation result of the reflection response of the entire medium fails to do so, due to the presence of interfering reflections from the overburden. Figure 2E, shows the correlation results for the first multiple (i.e. the blue zone in 2A-C). Since the wavefield traverses the reservoir for a second time, the actual time differences are now doubled. Furthermore, the multiple is masked by the underburden for response R^0_{bc}, hence solely the correlation of R^0_b resembles the true time difference. However, even in R^0_b the multiple energy is relatively low, and the correlation is unable to detect the time difference at some receiver locations.

DISCUSSION

Although the previous section showed promising results, there are some limitations and potential improvements to the methodology that will now be discussed.

First, the numerical data in this example is free of any kinds of noise, obviously this is not a realistic expectation for field data. The introduction of noise would especially interfere with capabilities of the frequency domain interpolation, deteriorating the results for the first arrival correlations. On the contrary, this could also increase the significance of the internal multiples, which can rely more on the coarse sampling rate as opposed to the interpolated results that are key for the primary reflection.

Another limitation is that solely the zero-offset traces are used, even though the full offsets are available. Therefore, the method is ideally extended to include all available offsets. Additionally, this would open the door to apply AVO analysis on the different responses, which is another useful tool in 4D seismic. These developments are subject to further research.

Lastly, repeatability of a survey is an important factor in time-lapse studies, because the acquisition geometry has a large impact on the recorded wavefield. We note that the wavefield redatuming steps of the method can possibly be exploited to account for irregularities in the acquisition geometry between the baseline and monitor study. This is twofold: for one Marchenko redatuming (Equation 3) removes all transmission effect from the overburden, and secondly the multidimensional deconvolution and extrapolation steps can be used to repair distortions in the acquisition geometry.

CONCLUSION

This work aimed to propose a method to resolve traveltime differences between a baseline and monitor survey in the presence of a strongly scattering overburden and underburden. In order to achieve this, the proposed method isolates the reservoir response from the reflection response of the full medium with the help of the Marchenko method. Next, the arrival times of the wavefield perturbed by the reservoir are computed, and a correlation window is defined. Finally, the time shift between the two studies is determined, by correlating the primary or multiple reflections of the baseline and the monitor study in this window.

The results obtained with a numerical example show a strong correlation between the actual traveltimes differences and the computed time differences of the responses without the overburden. On the contrary, the response that included the over-

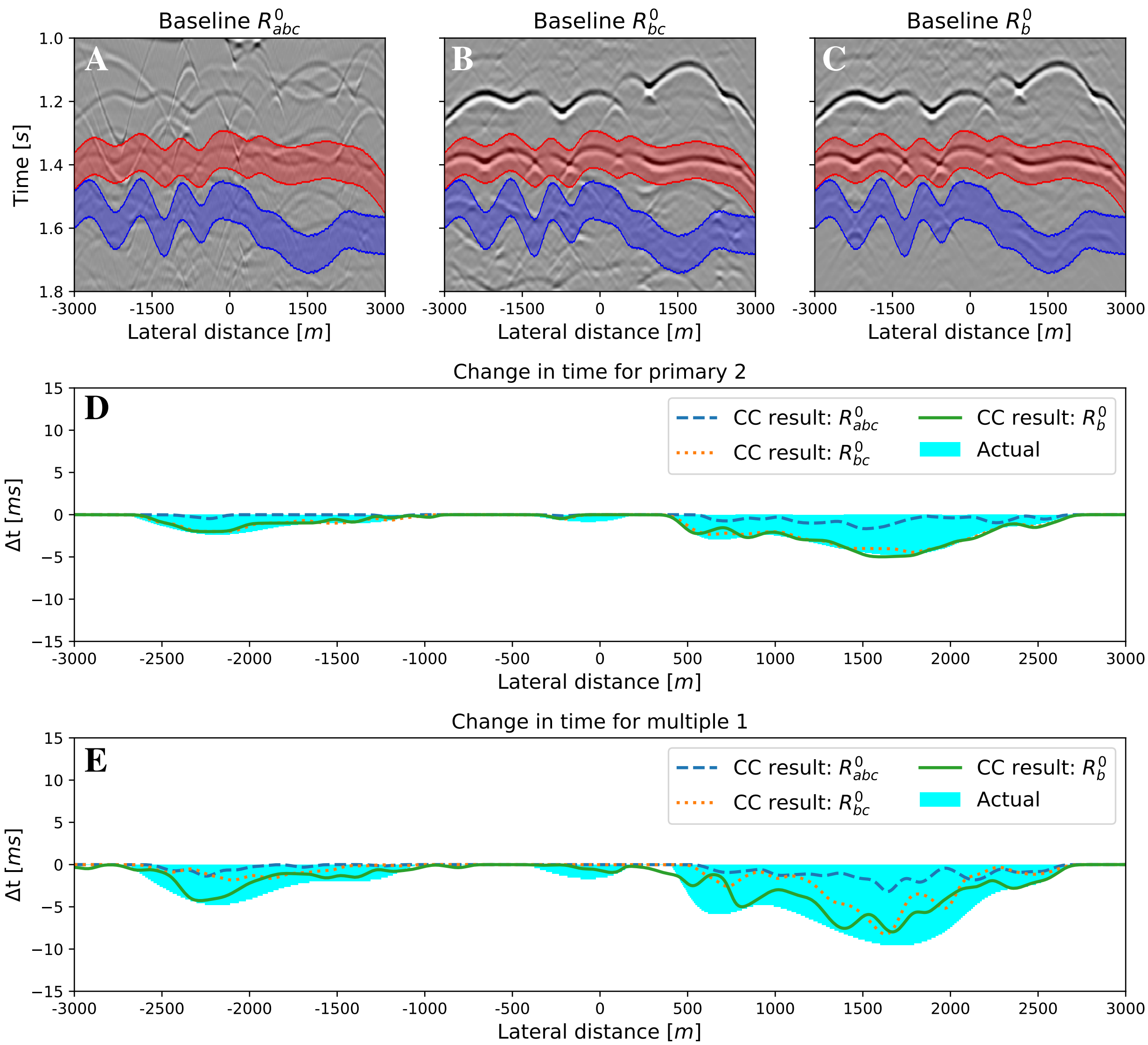

Figure 2: *The top row shows the baseline zero-offset reflection response of the entire medium R^0_{abc} (A), medium after overburden removal R^0_{bc} (B), medium after over- and underburden removal R^0_b (C). A 20 Hz Ricker wavelet has been applied to each response. The red and blue area mark the correlation window for the second primary arrival and the first multiple, respectively. The time-shifts determined from the cross-correlation between the baseline and monitor studies for the second primary are shown in D and the results for the first multiple are shown in E. The dashed blue line, the dotted orange line, and the solid green line display the result for responses R^0_{abc}, R^0_{bc} and R^0_b, respectively. The light blue area marks the real time difference at each offset.*

burden fails to produce the correct time differences. Furthermore, correlation of the primary reflection provides more accurate results compared to first internal multiple, even though the latter propagates through the reservoir multiple times.

In conclusion, the new methodology has the potential to more accurately observe traveltime differences in a reservoir, when its response is masked by over- and underburden effects, allowing for improved monitoring of changes inside subsurface reservoirs.

ACKNOWLEDGEMENTS

We thank Jan Thorbecke for his help with the numerical examples and fruitful discussions. Also, we acknowledge funding from the European Research Council (ERC) under the European Union's Horizon 2020 research and innovation programme (grant agreement No: 742703).